High-order harmonic generation in fullerenes using few- and multi-cycle pulses of different wavelengths

Rashid A. Ganeev,[1,2,*] Christopher Hutchison,[1] Tobias Witting,[1] Felix Frank,[1] Sébastien Weber,[1] William A. Okell,[1] Emilio Fiordilino,[3] Dario Cricchio,[3] Franco Persico,[3] Amelle Zaïr,[1] John W. G. Tisch,[1] and Jonathan P. Marangos[1]

[1]*Blackett Laboratory, Imperial College London, Prince Consort Road, London SW7 2AZ, UK*
[2]*Voronezh State University, Voronezh 394006, Russia*
[3]*University of Palermo, Physical Department, Via Archirafi 36, Palermo 90123, Italy*
**Corresponding author: rashid_ganeev@mail.ru*

Received August 10, 2012; revised October 23, 2012; accepted October 23, 2012; posted October 23, 2012 (Doc. ID 174103); published December 3, 2012

We present the results of experimental and theoretical studies of high-order harmonic generation (HHG) in plasmas containing fullerenes using pulses of different duration and wavelength. We find that the harmonic cutoff is extended in the case of few-cycle pulses (3.5 fs, 29th harmonic) compared to longer laser pulses (40 fs, 25th harmonic) at the same intensity. Our studies also include HHG in fullerenes using 1300 and 780 nm multicycle (35 and 40 fs) pulses. For 1300 nm pulses, an extension of the harmonic cutoff to the 41st order was obtained, with a decrease in conversion efficiency that is consistent with theoretical predictions based on wave packet spreading for single atoms. Theoretical calculations of fullerene harmonic spectra using the single active electron approximation were carried out for both few-cycle and multicycle pulses.

OCIS codes: 190.4160, 190.4180.

1. INTRODUCTION

Finding new approaches to improve the efficiency of high-order harmonic generation (HHG) of laser radiation toward the extreme ultraviolet (XUV) range is an important goal of nonlinear optics and laser physics. Small sized nanostructures are an attractive approach, since they exhibit local-field-induced enhancement of the nonlinear optical response of the medium [1–3]. Another mechanism that can enhance harmonic efficiency of clusters is the increase of the recombination cross section of accelerated electron and parent particle in the final step of the three-step mechanism of HHG [4]. It was shown in [5] that laser-irradiated cluster-contained plasmas can emit low-order harmonics efficiently. The advantages of highly efficient harmonic generation in laser-produced plasmas containing nanoparticles have been analyzed in [3].

Fullerenes are an attractive nonlinear medium for the HHG. Their relatively large sizes and broadband surface plasmon resonance (SPR) in the XUV range allowed the first demonstration of enhanced HHG near the SPR of C_{60} ($\lambda_{SPR} \approx 60$ nm, with 10 nm FWHM) [6]. Theoretical studies of HHG from C_{60} using multicycle pulses include an extension of the three-step model [7], analysis of the electron bound within a thin shell of a rigid spherical surface, with geometrical parameters similar to those of the C_{60} [8], and application of dynamical simulations [9]. Those studies reveal how HHG can be used to probe the electronic and molecular structure of C_{60}. Theoretical investigation of such systems is hampered by the fact that the Hamiltonian of HHG is time dependent and the systems consist of many electrons. The investigation of the influence of the electrons on the resonant HHG can be performed by means of a multiconfigurational time-dependent Hartree–Fock (MCTDHF) approach, which has the accuracy of direct numerical solution of the Schrödinger equation and is not significantly more complicated than the ordinary time-dependent Hartree–Fock approach [10]. In particular, the computations could be based on the multiconfigurational time-dependent Hartree software packages [11]. In [10], simulations of resonant HHG were performed by means of a MCTDHF approach for three-dimensional fullerene-like systems. The influence of the SPR of C_{60} on the harmonic efficiency in the range of 60 nm ($E = 20$ eV) was analyzed and showed the role of resonant effects in the HHG enhancement.

The ionization saturation intensities of different charge states of C_{60} are higher compared to isolated atoms of similar ionization potential [12]. With this perspective, it is interesting to analyze HHG from fullerene molecules in the field of few-cycle laser pulses and compare these studies with those carried out using multicycle pulses. The motivation for the present work was to analyze the conditions for efficient HHG from plasmas containing C_{60}, using picosecond laser pulses to ablate the fullerene-containing target at high pulse repetition rate (1 kHz) and then few-cycle laser pulses ($\tau = 3.5$ fs) to generate the harmonics in the fullerene plasma. We also investigated HHG in fullerenes using 1300 nm radiation and compared these studies with those using 780 nm multicycle pulses. We employed a new technique that led to a considerable improvement in the stability of the harmonics from the plasma produced on the fullerene-containing targets, which is crucial in high pulse repetition rate experiments. We also carried out a theoretical study of fullerene plasma HHG.

2. RESULTS AND DISCUSSION

A small part ($E = 120$ μJ) of the uncompressed radiation of a 1 kHz chirped pulse amplification Ti:sapphire laser (Femtolasers Produktions GmbH) with central wavelength 780 nm and pulse duration 8 ps was split from the beam line

prior to the laser compressor stage and was focused into the vacuum chamber to create a plasma on the C_{60}-containing target using an intensity on the target surface of typically $I_{ps} = 2 \times 10^{10}$ W cm^{-2} (Fig. 1). The Ti:sapphire laser after compression provided pulses of 30 fs duration and energies of up to 0.8 mJ. The amplified pulses were focused into a 1 m long differentially pumped hollow core fiber filled with neon. The spectrally broadened pulses at the output of the fiber were compressed by 10 bounces of double-angle technology chirped mirrors. A pair of fused silica wedges was used to fine tune the pulse compression. In this way, high-intensity 3.5 fs pulses were generated.

These few-cycle pulses were focused into the plasma plume, approximately 150–200 μm above the target surface, to generate high-order harmonics using a 400 mm focal length reflective mirror. The delay between plasma initiation and the arrival at the plume of the few-cycle pulse was fixed at 34 ns, which optimized harmonic emission. The plasma plume and target were moved over a range of positions with respect to the focal point of the few-cycle pulse, to optimize the conversion efficiency of harmonic generation. The laser intensity in the plume was $I_{fs} = 5 \times 10^{14}$ W cm^{-2}. The HHG radiation was analyzed by an XUV spectrometer consisting of a flat-field grating (1200 lines /mm, Hitachi) and an imaging microchannel plate detector (Photonis USA, Inc.) read out by a CCD camera. We investigated two types of targets: (i) C_{60} powder, which was glued onto a glass substrate or onto a rotating aluminium rod and (ii) bulk graphite for plasma harmonic generation. The maximum harmonic conversion efficiency was obtained by varying the distance between the femtosecond beam and the target, as well as the z-position of the plasma. The harmonic spectra from plasmas produced on the bulk graphite and fullerene powder glued onto the glass surface are presented in Fig. 2(a) in the case of laser wavelength $\lambda = 780$ nm. Harmonics up to the 29th order were obtained from the fullerene plasma. Note that the harmonic efficiency in the case of the graphite plasma was about 5 times higher compared with the case of fullerene plasmas, most likely due to the higher concentration of emitters in the former case, as has also been reported in [13].

Here we also present the results of comparative studies of the HHG in fullerene plasma using few-cycle (3.5 fs) and multicycle (40 fs) pulses [Fig. 2(b)] of 780 nm radiation. In the latter case, we used a 1 kHz repetition rate Ti:sapphire laser (Red Dragon, KML Inc.) generating 4 mJ, 40 fs pulses, which were

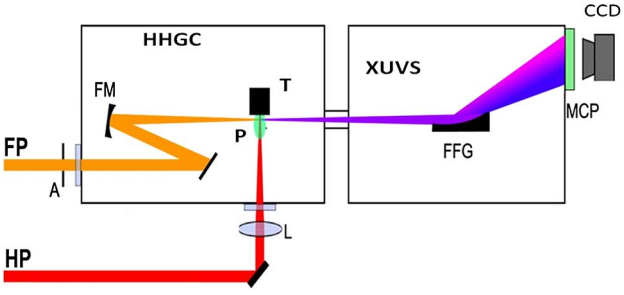

Fig. 1. (Color online) Experimental setup for harmonic generation in plasma. FP, femtosecond probe pulse; HP, picosecond heating pulse; A, aperture; HHGC, high-order harmonic generation chamber; FM, focussing mirror; L, focussing lens; T, target; P, plasma; XUVS, extreme ultraviolet spectrometer; FFG, flat field grating; MCP, microchannel plate and phosphor screen detector; CCD, CCD camera.

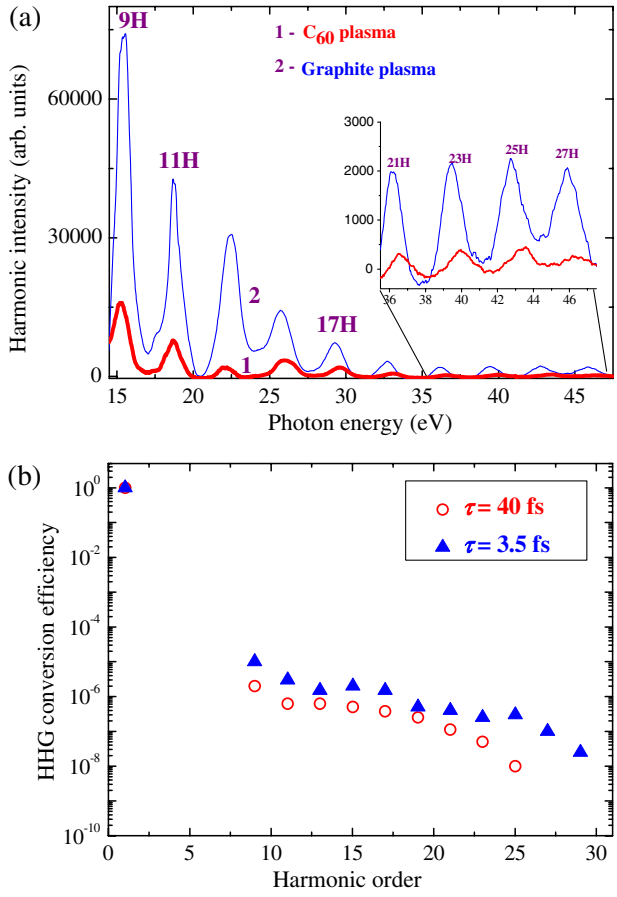

Fig. 2. (Color online) (a) Harmonic spectra from fullerene (thick curve) and graphite (thin curve) plasmas using the heating 8 ps pulses and 3.5 fs probe pulses at identical experimental conditions. (b) Comparison of HHG conversion efficiencies from fullerene plasma using the 3.5 fs (triangles) and 40 fs (circles) probe pulses. Here the laser wavelength is $\lambda = 780$ nm.

used for the HHG in various laser plasmas. The HHG conversion efficiency for the 40 fs pulses at the beginning of plateau range in the case of the plasma plume containing fullerenes was estimated to be $\sim 5 \times 10^{-6}$ using a comparison with the HHG conversion efficiency in a silver plasma, which has previously been reported at similar experimental conditions to be 1×10^{-5} [3]. One can note that the cutoff in the case of longer pulses (25th harmonic) was shorter with regard to the few-cycle pulses at similar intensities of these pulses in the plasma plume.

The problem with using a fullerene powder-containing target is the shot-to-shot instability and rapid decrease of the harmonic yield, due to the abrupt change in the target morphology following ablation. Such instabilities limit applications of this radiation source and greatly hamper efforts to measure the pulse duration of the harmonic emission, which typically requires a large number of laser shots. A solution to this problem might be the use of long homogeneous tapes containing fullerenes, which continuously move from shot to shot to provide a fresh surface for each next laser pulse. The use of rotating targets containing C_{60} is another method for improvement of the harmonic stability [14] from this medium, which was implemented in this work. We used 15 mm diameter aluminium rods as the substrates onto which the fullerene powder was glued. These rotating targets considerably improved the stability of harmonics from C_{60}-containing plasmas

compared with fixed targets fabricated by gluing fullerene powder to a glass substrate. We found that once the target rotation is stopped, the harmonic efficiency from the fullerene plasma decreased to the noise level within 1–2 s.

This target fabrication method could be very useful in the case of powder-like targets (fullerenes, metal nanoparticles, organic powder-like samples). Previously, even at 10 Hz pulse repetition rate, the ablation of powdered targets that were not moved led to their rapid degradation and abrupt decrease of harmonic yield [3]. With this new technique, one can glue the powdered material onto the rotating rod to improve the stability of the harmonic emission. At the same time, one can note that the stability of harmonics from such powder-like targets is still worse than from rotating bulk metal rods due to the faster degradation of the target surface in the former case.

We did not estimate the density of fullerenes on the rotating target. In principle, it should be the same as the density of powder, since we just glued the fullerene powder without additional pressing. The thickness of powder layer was 2 mm. The uniformity was maintained with the accuracy better that 0.1 mm.

Due to small concentration of fullerenes in the plasma plume, the amount of ablated material was insignificant even at 1 kHz pulse repetition rate. So the main difference between the rotating and nonrotating targets was the thermal conditions of heating spot. In the case of fixed target, the melting bath appeared after 1000 shots (e.g., 1 s of ablation), which considerably worsened the process of plasma formation. Once the target started to move, the previously heated area cooled down and again could be used for efficient ablation and harmonic generation. We observed this phenomenon from many targets. So here we were able to improve the stability of harmonics (and correspondingly stability of plasma formation conditions) not just by using the fresh (nonablated) surface but by changing the conditions of overheating of the same spot of the target. Based on our experiments with different (rotating and fixed) targets we concluded that the overheating of the same spot worsens the conditions for stable plasma formation. The morphology of the heating spot did not remain intact during these experiments. At the same time the creation of craters in the case of rotating target occurred after considerably longer period compared with static targets.

Conversion efficiency studies in these two plasmas showed advantages of HHG in the case of graphite plasmas compared with fullerene plasmas [13]. This can be explained by the higher particle density in the graphite plasma. The concentration of fullerenes is below 10^{17} cm^{-3} [6], while our density estimates for carbon plasmas based on a three-dimensional molecular dynamical simulation of laser ablation of graphite using the molecular dynamics code ITAP IMD [15] showed that for heating by 8 ps laser pulses the graphite plasma density can reach 2.6×10^{17} cm^{-3} at the moderate ablation intensity of 2×10^{10} W cm^{-2}. Another reason for the observed superior features of graphite plasma harmonics could be the production of clusters during laser ablation, though their involvement in HHG requires additional studies, including time-of-flight measurements.

In order to analyze the harmonic yield from the fullerene plasma using the mid-infrared (MIR) laser source, we used an optical parametric oscillator (OPO) pumped by the 40 fs Ti:sapphire laser. A beam splitter inserted before the laser compressor of this Ti:sapphire laser was used to pick off 10% of the beam (780 nm, 1 mJ, 160 ps, 1 kHz pulses) to generate a fullerene-containing plasma plume, with the remaining 90% being compressed to 40 fs (7 mJ) to pump a commercial computer-controlled OPO (HE-TOPAS, Light Conversion). The OPO was optimized for high conversion efficiency, beam quality and short duration of the converted pulses. The OPO provided signal pulses with duration of 35 fs in the 1200–1600 nm spectral range with a maximum energy of 1.7 mJ at ~1300 nm. The idler pulses covered the 1600–2200 nm range with a maximum energy of 1 mJ at ~2000 nm. The delay between the heating ablation pulse and MIR pulse from the OPO was set to 35 ns, as this delay was found to be optimal for the efficient generation of extended harmonics from fullerene plasma.

Figure 3 shows the comparison of fullerene harmonic spectra generated in the case of 1300 and 780 nm multicycle probe pulses. Harmonics up to the 41st order (Fig. 3, bottom panel) were observed in the case of 1300 nm probe pulses at the conditions of optimal plasma formation using the heating 160 ps pulses. The application of less intense, longer wavelength (1400 nm) pulses available by tuning the OPO did not result in an extension of harmonic cutoff compared with the case of probe 1300 nm pulses. This observation suggests that the harmonic generation occurred under saturated conditions, with the expectation of stronger harmonics once the microprocesses and macroprocesses governing frequency conversion are optimized. Overexcitation of target by 160 ps pulses (Fig. 3, middle panel) led to appearance of plasma emission in the

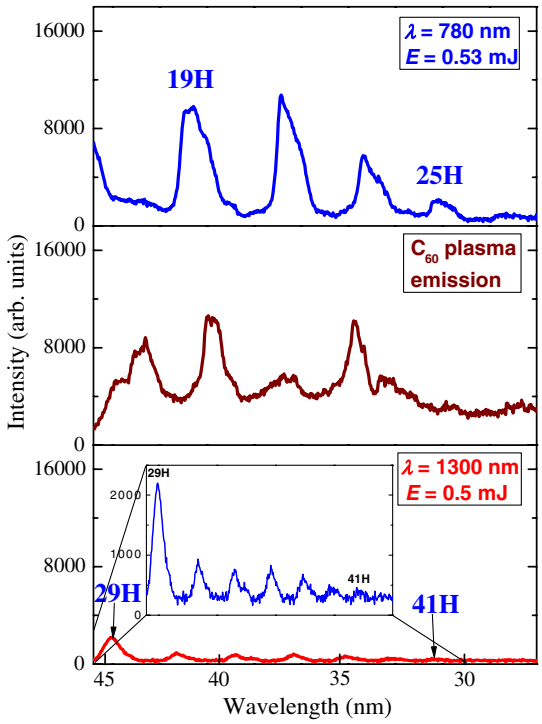

Fig. 3. (Color online) Comparative harmonic spectra from fullerene-contained plume using the 780 nm (upper panel) and 1300 nm (bottom panel) multicycle pulses (intensity of heated 160 ps pulses $I_{ps} = 1 \times 10^{10}$ W cm^{-2}). The intensity axes are on the same scale allowing a direct comparison between the three cases. The middle panel shows C_{60} plasma emission spectrum at overexcitation of target by 20 ps pulses ($I_{ps} = 4 \times 10^{10}$ W cm^{-2}), without further excitation by femtosecond probe pulses.

25–45 eV range of photon energies ($\lambda = 27$–50 nm). At these conditions, no harmonics were observed during propagation of femtosecond pulses through such overexcited plasma.

The harmonic spectrum up to the 25th order in the case of 780 nm, 40 fs probe pulses is presented in Fig. 3 (upper panel). One can clearly see the extension of harmonic cutoff (from the point of view of highest harmonic order) in the case of longer-wavelength probe pulses by comparing the HHG spectra using the 780 and 1300 nm probe pulses, while the extension of cutoff energy was insignificant.

We maintained approximately equal energies of driving pulses in these cases (0.53 mJ for 780 nm pulses and 0.5 mJ for 1300 nm pulses). The intensity of 780 nm radiation in the plasma area was calculated to be $I_{fs} = 4 \times 10^{14}$ W cm^{-2}. The pulse durations of these sources (780 and 1300 nm) were approximately the same (40 and 35 fs, respectively). Probably due to phase modulation and propagation through multiple optical elements in optical parametric oscillator-amplifier, the diameter of a 1300 nm beam in the plasma plume was bigger than in the case of a 780 nm beam. The corresponding lower intensity of 1300 nm radiation could be responsible for less expected extension of harmonic cutoff energy. From the cutoff formula, we could expect the generation of harmonics up to the 47th order (in the case of 780 nm radiation), well above the observed cutoff (25th harmonic), which probably points out the difference in expected and actual intensity in the plasma area at the optimal conditions of HHG. The reason for this discrepancy could be related to the self-defocusing of driving pulses in the medium containing free electrons. Below we also discuss the cutoff law and its limit of validity at our experimental conditions.

In atoms the maximum emitted photon energy (giving the cutoff position) is described by the well-known relation $E_M = I + 3.17U_p$ with I the ionization energy and U_p the ponderomotive energy. By invoking the three-step model [4] this formula can be derived (by use of mere energy conservation and Newton laws) under the assumptions that the laser field amplitude is constant. Rapidly varying laser pulses can considerably shift the cutoff [16,17]. We also know that molecules support more returning trajectories than atoms and allow the existence of several plateau [18]; it is not therefore easy to disentangle the effects of pulse shape and presence of a molecule and to state a general law for the position of the cutoff; the $E_M = I + 3.17U_p$ law can therefore be used only as a touchstone.

We observed that the plasma harmonic yields from the 780 and MIR probe pulses are consistent with the predicted single-atom harmonic intensity wavelength scaling $I_h \propto \lambda^{-5}$, which arises due to electron wave packet spreading before recollision [19,20]. The harmonic efficiency of the XUV radiation in the range of 30–50 nm driven by MIR pulses was 7–15 times less compared with the case of 780 nm probe pulses, which is comparable with the expected ratio between harmonic intensities from these sources ($(1300/780)^5 \approx 12.7$) followed from above rule, assuming approximately equal energies of the 780 and 1300 nm pulses (0.53 and 0.5 mJ, respectively).

The fact that HHG in the fullerene system exhibits a wavelength scaling that is consistent with single-atom predictions encouraged us to employ a theoretical model [21] in which the interaction of short pulses with C_{60} was treated in the single active electron approximation with one electron constrained over a structureless spherical surface of radius $R = 3.55 \times 10^{-8}$ cm $= 6.71a_0$. This simplified model can be treated in an analytical fashion. It permits a physical understanding of the dynamics of the active electron, and allows an easy check of resonances between bare molecular state. Indeed a generalization of the model can be used to analyze the physical properties, the energy content, and stability of hollow spherical clusters [22]. The calculated harmonic spectra from C_{60} are presented in Fig. 4 in the case of 780 nm (photon energy $E_{ph} = 1.6$ eV) and 1300 nm (photon energy $E_{ph} = 0.96$ eV) pulses propagating through the fullerene medium. The calculations were carried out for 2-cycle pulses ($t = 5.2$ fs) and 12-cycle pulses ($t = 31$ fs) of 780 nm radiation and 8-cycle pulses ($t = 34$ fs) of 1300 nm radiation and

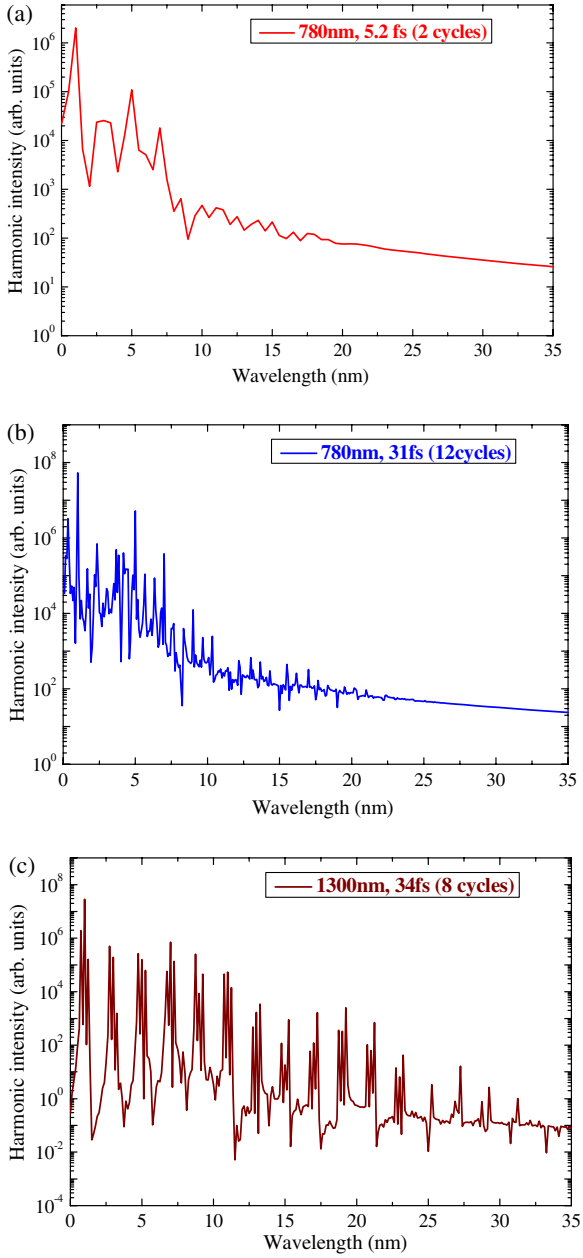

Fig. 4. (Color online) Calculated data of the harmonic spectra from fullerene plasma in the case of (a), (b) 780 nm and (c) 1300 nm probe radiation. The pulse durations are (a) 2 optical cycles (5.2 fs), (b) 12 optical cycles (31 fs), and (c) 8 optical cycles (34 fs).

intensity 6×10^{14} W cm^{-2}, which were close to the conditions of fullerene HHG experiments.

The spectra are formed of well-resolved harmonics but with broadened lines (in the case of short pulses) and hyper Raman lines (in the case of long pulses). Hyper Raman, lines with frequency other than harmonics, are due to transitions between laser dressed molecular states [23,24]. The presence of these lines has been predicted since the very beginning of the theoretical treatment of HHG [25] and found in different contexts, such as two-level approximation, quantum dots calculations, hydrogen atom, and so on [26–29], but never observed in actual experiments. Several explanations have been proposed to explain this failure; for example, it has been argued that they add destructively in the forward direction or that they show a transient nature and are thus overwhelmed by the presented odd harmonics [30,31].

Our calculations showed well-defined harmonics (up to $H_c = 31$) in the case of 1300 nm multicycle pulses. The theoretical model exploited the spherical symmetry of the C_{60} by introducing a number of approximations, the most important of which is that the molecule cannot be ionized. This approximation deserves some comment. In spite of the ionization suppression of the C_{60} molecule, some ionization is bound to occur so that the theory becomes unreliable when ionization becomes significant. The harmonic cutoff in the case of 1300 nm radiation was extended compared with 780 nm radiation ($H_c = 17$), analogously as in the case of experiment.

Previous HHG studies in fullerenes were performed using the multicycle pulses (30, 48, and 110 fs [3]). The stability of C_{60} against fragmentation in multicycle laser fields leads to fast diffusion of the excitation energy. Even better conditions can occur in the case of few-cycle pulses used for fullerene HHG. In that case fullerenes can withstand the influence of the strong field of few-cycle pulses due to the increase of the ionization saturation intensity as the pulse duration is decreased. This can further increase the diffusion of the excitation energy within the fullerenes due to their very large number of internal degrees of freedom. The increase of energy diffusion is expected to lead to a decrease in the disintegration of fullerenes, which enhances the probability of harmonic emission from these molecules.

The graphite plasmas, which were compared in our experiments with C_{60}, can easily be aggregated during laser ablation, thus leading to nanoparticles in the laser plume. In that case the comparison of two clustered species (large 5–20 nm carbon clusters and 0.7 nm C_{60}) can lead to their different nonlinear optical response once the interacting laser pulse becomes compressed from the multicycle to few-cycle duration. Our results show that for the shortest laser pulses, the HHG cutoff for fullerene is extended, while the harmonic intensity is reduced compared with "carbon harmonics." The intensity of the probe femtosecond pulse is an important parameter for optimizing the HHG from C_{60}. Increasing the intensity of the probe pulse did not lead to an extension of the harmonic cutoff from the fullerene plume, which is a signature of HHG saturation in the medium. Moreover, at relatively high probe intensities, we observed a decrease in the harmonic output, which can be attributed to the phase mismatch caused by propagation effects.

The stability of C_{60} molecules against ionization and fragmentation is of particular importance, especially for their application as a medium for HHG using laser pulses of different duration. The fullerene molecules ablated off the surface should be intact when the probe pulse arrives. Hence, the heating pulse intensity also becomes a sensitive parameter. At lower intensities the concentration of the clusters in the plume would be low, while at higher intensities one can expect fragmentation. This phenomenon is observed when the heating pulse intensity on the surface of fullerene-rich targets is increased above the critical value (Fig. 3, middle panel). The abrupt reduction in harmonic intensity in that case can be attributed to phenomena such as fragmentation of fullerenes, an increase in free electron density, and self-defocusing of the probe laser, all of which are expected to reduce the efficiency of HHG.

3. CONCLUSIONS

We presented the results of the experimental and theoretical studies of HHG in the plasmas containing fullerenes (up to the 29th and 41st orders for the 780 and 1300 nm probe radiation) under different plasma conditions and laser parameters in the case of few-cycle and multicycle pulses. The comparison of harmonics from C_{60}-rich plasmas and plasmas produced on graphite surface showed stronger harmonic yield in the latter case, which was attributed to higher density of the plasma plume and the formation of clusters during the ablation of graphite targets. Our experiments with fullerene powder glued onto aluminium rotating rods demonstrated a dramatic improvement in harmonic generation stability compared with static fullerene-containing targets. Our comparative studies using 3.5 and 40 fs pulses showed that, for few-cycle pulses, the harmonic cutoff is extended compared with multicycle pulses, which can be attributed to reduced fragmentation of C_{60} for the shorter pulse. The comparison of fullerene harmonic spectra generated in the case of 1300 and 780 nm multicycle probe pulses showed the extension of generating harmonic orders in the former case. The plasma harmonic yield approximately follows the $I_h \propto \lambda^{-5}$ wavelength scaling rule predicted for single atoms. The maximal conversion efficiency obtained in these fullerene HHG studies was estimated to be 5×10^{-6}. Theoretical calculations of fullerene harmonic spectra were carried out in the single active electron approximation, which showed harmonics up to $H_c = 31$ in the case of 1300 nm multicycle pulses and up to $H_c = 17$ in the case of 780 nm multicycle pulses.

ACKNOWLEDGMENTS

This research was supported by EPSRC programme (grants EP/F034601/1, EP/I032517/1, and EP/E028063/1). R. A. Ganeev acknowledges support from the Marie Curie International Incoming Fellowship Grant within the 7th European Community Framework Programme (grant PIIF-GA-2009-253104). The authors thank G. Castiglia for comments on the numerical calculations.

REFERENCES

1. T. D. Donnelly, T. Ditmire, K. Neuman, M. D. Perry, and R. W. Falcone, "High-order harmonic generation in atom clusters," Phys. Rev. Lett. **76**, 2472–2475 (1996).
2. C. Vozzi, M. Nisoli, J.-P. Caumes, G. Sansone, S. Stagira, S. De Silvestri, M. Vecchiocattivi, D. Bassi, M. Pascolini, L. Poletto, P. Villoresi, and G. Tondello, "Cluster effects in high-order

harmonics generated by ultrashort light pulses," Appl. Phys. Lett. **86**, 111121 (2005).
3. R. A. Ganeev, "Harmonic generation in laser-produced plasma containing atoms, ions and clusters: a review," J. Mod. Opt. **59**, 409–439 (2012).
4. P. B. Corkum, "Plasma perspective on strong-field multiphoton ionization," Phys. Rev. Lett. **71**, 1994–1997 (1993).
5. S. V. Popruzhenko, D. F. Zaretsky, and D. Bauer, "Energy absorption and emission of harmonics by clusters subject to intense short laser pulses," Laser Phys. Lett. **5**, 631–646 (2008).
6. R. A. Ganeev, L. B. Elouga Bom, J. Abdul-Hadi, M. C. H. Wong, J. P. Brichta, V. R. Bhardwaj, and T. Ozaki, "Higher-order harmonic generation from fullerene by means of the plasma harmonic method," Phys. Rev. Lett. **102**, 013903 (2009).
7. M. F. Ciappina, A. Becker, and A. Jaron-Becker, "Multislit interference patterns in high-order harmonic generation in C_{60}," Phys. Rev. A **76**, 063406 (2007).
8. M. Ruggenthaler, S. V. Popruzhenko, and D. Bauer, "Recollision-induced plasmon excitation in strong laser fields," Phys. Rev. A **78**, 033413 (2008).
9. G. P. Zhang, "Optical high harmonic generation in C_{60}," Phys. Rev. Lett. **95**, 047401 (2005).
10. P. V. Redkin and R. A. Ganeev, "Simulation of resonant high-order harmonic generation in three-dimensional fullerenelike system by means of multiconfigurational time-dependent Hartree-Fock approach," Phys. Rev. A **81**, 063825 (2010).
11. H.-D. Meyer, U. Manthe, and L. S. Cederbaum, "The multi-configurational time-dependent Hartree approach," Chem. Phys. Lett. **165**, 73–78 (1990).
12. V. R. Bhardwaj, P. B. Corkum, and D. M. Rayner, "Recollision during the high laser intensity ionization of C_{60}," Phys. Rev. Lett. **93**, 043001 (2004).
13. Y. Pertot, L. B. Elouga Bom, V. R. Bhardwaj, and T. Ozaki, "Pencil lead plasma for generating multimicrojoule high-order harmonics with a broad spectrum," Appl. Phys. Lett. **98**, 101104 (2011).
14. C. Hutchison, R. A. Ganeev, T. Witting, F. Frank, W. A. Okell, J. W. G. Tisch, and J. P. Marangos, "Stable generation of high-order harmonics of femtosecond laser radiation from laser produced plasma plumes at 1 kHz pulse repetition rate," Opt. Lett. **37**, 2064–2066 (2012).
15. J. Roth, F. Gähler, and H.-R. Trebin, "A molecular dynamics run with 5 180 116 000 particles," J. Mod. Phys. C **11**, 317–322 (2000).
16. E. Fiordilino and V. Miceli, "Laser pulse shape effects in harmonic generation from a two-level atom," J. Mod. Opt. **41**, 1415–1426 (1994).
17. J. Zhou, J. Peatross, M. M. Murnane, H. C. Kapteyn, and I. P. Christov, "Enhanced high-harmonic generation using 25 fs laser pulses," Phys. Rev. Lett. **76**, 752–755 (1996).
18. M. Lein, "Mechanisms of ultrahigh-order harmonic generation," Phys. Rev. A **72**, 053816 (2005).
19. J. Tate, T. Auguste, H. G. Muller, P. Saliéres, P. Agostini, and L. F. DiMauro, "Scaling of wave-packet dynamics in an intense midinfrared field," Phys. Rev. Lett. **98**, 013901 (2007).
20. K. Schiessl, K. L. Ishikawa, E. Persson, and J. Burgdörfer, "Quantum path interference in the wavelength dependence of high-harmonic generation," Phys. Rev. Lett. **99**, 253903 (2007).
21. D. Cricchio, P. P. Corso, E. Fiordilino, G. Orlando, and F. Persico, "A paradigm of fullerene," J. Phys. B **42**, 085404 (2009).
22. D. Cricchio, E. Fiordilino, and F. Persico, "Electrons on a spherical surface: physical properties and hollow spherical clusters," Phys. Rev. A **86**, 013201 (2012).
23. N. Moiseyev and M. Lein, "Non-Hermitian quantum mechanics for high-order harmonic generation spectra," J. Phys. Chem. A **107**, 7181–7188 (2003).
24. Z.-Y. Zhou and J.-M. Yuan, "Strengthened hyper-Raman lines with the coherent superposition state," Chin. Phys. Lett. **24**, 683–686 (2007).
25. T. Millack and A. Maquet, "Hyper-Raman lines produced during high harmonic generation," J. Mod. Opt. **40**, 2161–2171 (1993).
26. F. I. Gauthey, C. H. Keitel, P. L. Knight, and A. Maquet, "Role of initial coherence in the generation of harmonics and sidebands from a strongly driven two-level atom," Phys. Rev. A **52**, 525–540 (1995).
27. W. Chu, Y. Xie, S. Duan, N. Yang, W. Zhang, J.-L. Zhu, and X.-G. Zhao, "Model of generating either odd or even optical harmonics by varying the coupling parameters between source quantum dots," Phys. Rev. B **82**, 125301 (2010).
28. Z.-Y. Zhou and J.-M. Yuan, "Fine structures of the harmonic and hyper-Raman spectrum of the hydrogen atom in an intense high-frequency laser pulse," Phys. Rev. A **77**, 063411 (2008).
29. V. Kapoor and D. Bauer, "Floquet analysis of real-time wave functions without solving the Floquet equation," Phys. Rev. A **85**, 023407 (2012).
30. A. Di Piazza and E. Fiordilino, "Why hyper-Raman lines are absent in high-order harmonic generation," Phys. Rev. A **64**, 013802 (2001).
31. A. D. Bandrauk, S. Chelkowski, and H. S. Nguyen, "Nonlinear photon processes in molecules at high intensities-route to XUV—attosecond pulse generation," J. Mol. Struct. **735–736**, 203–209 (2005).